Front. Energy 2015, 9(3): 322–334
DOI 10.1007/s11708-015-0362-x

RESEARCH ARTICLE

Saeed VAFAEI, Alireza REZVANI, Majid GANDOMKAR, Maziar IZADBAKHSH

Enhancement of grid-connected photovoltaic system using ANFIS-GA under different circumstances

Abstract In recent years, many different techniques are applied in order to draw maximum power from photovoltaic (PV) modules for changing solar irradiance and temperature conditions. Generally, the output power generation of the PV system depends on the intermittent solar insolation, cell temperature, efficiency of the PV panel and its output voltage level. Consequently, it is essential to track the generated power of the PV system and utilize the collected solar energy optimally. The aim of this paper is to simulate and control a grid-connected PV source by using an adaptive neuro-fuzzy inference system (ANFIS) and genetic algorithm (GA) controller. The data are optimized by GA and then, these optimum values are used in network training. The simulation results indicate that the ANFIS-GA controller can meet the need of load easily with less fluctuation around the maximum power point (MPP) and can increase the convergence speed to achieve the MPP rather than the conventional method. Moreover, to control both line voltage and current, a grid side P/Q controller has been applied. A dynamic modeling, control and simulation study of the PV system is performed with the Matlab/Simulink program.

Keywords photovoltaic system, maximum power point (MPP), adaptive neuro-fuzzy inference system (ANFIS), genetic algorithm (GA)

1 Introduction

Among the alternative sources, the PV systems is considered as a natural energy source that is more useful, since it is clean, plentiful, free and participates as a main element of all other procedures of energy production in the world. To track the incessantly diverging MPP of the solar array, the maximum power point tracking (MPPT) control method plays a significant part in the PV arrays [1,2]. To control maximum output power, it is highly recommended that the MPPT system be used [3].

The most prevalent techniques are the perturbation and observation (P&O) algorithm [3,4], incremental conductance (IC) [5,6], fuzzy logic [7,8] and artificial neural networks (ANN) [9–11]. P&O and IC can track the MPP all the time, regardless of the atmospheric conditions, type of PV panel, by processing real values of PV voltage and current. Due to the aforementioned inquiries, the profits of P&O and IC methods are low cost execution and elementary method. One of the drawbacks of these techniques, however, is the vast variation of output power around the MPP even under steady-state, which lead to the loss of available energy more than other methods [12,13]. The rapid changing of weather condition affects the output power, making these methods unable to easily track the MPP.

Using fuzzy logic can dramatically solve the two problems mentioned. In fact, fuzzy logic controller can reduce oscillations of output power around the MPP and losses. Furthermore, in this way, convergence speed is higher than the other two ways mentioned. A weakness of fuzzy logic in comparison with ANN refers to oscillations of output power around the MPP [14,15].

Nowadays, artificial intelligence (AI) methods have numerous applications in determining the size of PV systems, MPPT control and optimal structure of PV systems. In most cases, multilayer perceptron (MLP) neural networks or radial basis function network (RBFN) are employed for modeling PV module and MPPT controller in PV systems [10–12,16–18].

The ANN can be considered as a robust technique for mapping the inputs-outputs of nonlinear functions, but it lacks subjective sensations and acts as a black box. On the other hand, fuzzy logic has the ability to transform linguistic and mental data into numerical values. However,

Received September 3, 2014; accepted December 19, 2014

Saeed VAFAEI (✉), Alireza REZVANI, Majid GANDOMKAR,Maziar IZADBAKHSH
Department of Electrical Engineering, Saveh Branch, Islamic Azad University, Saveh, Iran
E-mail: s.vafaei.elect@gmail.com

the determination of membership functions and fuzzy rules depends on the previous knowledge of the system. Neural networks can be integrated with fuzzy logic and through the combination of these two smart tools, a robust AI technique called adaptive neuro-fuzzy inference system (ANFIS) can be obtained [19–21].

GA is used for data optimization and then, the optimum values are utilized for training neural networks and the results show that the GA technique has less fluctuation in comparison with the conventional methods [22–24]. However, one of the major drawbacks in the papers mentioned that they are not practically connected to the grid in order to ensure the analysis of PV system performance.

In this paper, first, the 360 data of temperature and irradiance as the input data are given to GA and optimal voltage (V_{MPP}) corresponding to the MPP delivery from the PV system. Then the optimum values are utilized for training the ANFIS.

2 Photovoltaic cell mode

Figure 1 shows the equivalent circuit of a PV array [2,3]. The characteristic of the solar array is explained as

$$I_{PV} = I_d + I_{RP} + I, \tag{1}$$

$$I = I_{PV} - I_0\left[\exp\left(\frac{V + R_S I}{V_{th} n}\right) - 1\right] - \frac{V + R_s I}{R_P}, \tag{2}$$

$$V_{th} = \frac{N_s K T}{q}, \tag{3}$$

$$I_0 = I_{0,n}\left(\frac{T_n}{T}\right)^3 \exp\left[\frac{qE_g}{nK}\left(\frac{1}{T_n} - \frac{1}{T}\right)\right], \tag{4}$$

where I is the output current, V is the output voltage, I_{PV} is the generated current under a given insolation, I_d is the diode current, I_{RP} is the shunt leakage current, I_0 is the diode reverse saturation current, n is the ideality factor (1.36) for a *p-n* junction, R_s is the series loss resistance (0.1 Ω), R_P is the shunt loss resistance (161.34 Ω), and V_{th} is known as the thermal voltage. q is the electron charge ($1.60217646 \times 10^{-19}$ C), K is the Boltzmann constant ($1.3806503 \times 10^{-23}$ J/K) and T (Kelvin) is the temperature of the *p-n* junction. E_g is the band gap energy of the semiconductor ($E_g \approx 1.1$ eV for the polycrystalline Si at 25°C), $I_{0,n}$ is the nominal saturation current, T is the cell temperature and T_n is the cell temperature at reference conditions. Red sun 90 W is implemented as the reference module for simulation and the name-plate details are listed in Table 1. The array is the combination of 7 cells in series and 7 cells in parallel of the 90 W modules; accordingly, the array generates 4.4 kW.

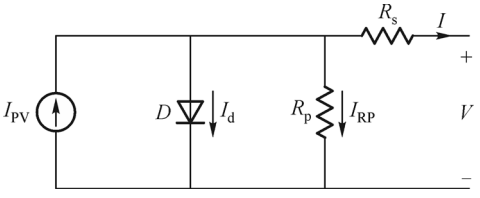

Fig. 1 Equivalent circuit of the photovoltaic array

3 GA Technique and ANFIS

3.1 Steps of implementing GA

The GA based offline trained ANFIS is employed to provide the reference voltage corresponding to the maximum power. Alongside, GA is utilized for optimum values which are then used for training ANFIS [22–24]. The procedure employed for implementing GA is as follows [22–25]: Assigning the objective function and recognizing the design parameters; determining the initial production population; evaluating the population using the objective function; and conducting convergence test stop if convergence is provided.

The objective function of GA is employed for its optimization by finding the optimum $X = (X_1, X_2, ..., X_n)$ to put the $F(X)$ in the maximum value, where the number of design variables are considered as 1, where X is the design variable equal to array current (I_X) and $F(X)$ is the array output power which should be maximized [22]. The GA parameters are tabulated in Table 2. The correlation between the voltage and current of the array can be expressed as

$$F(X) = V_X I_X, \tag{5}$$

$$0 < I_X < I_{SC}. \tag{6}$$

By maximizing this function, the optimum values for V_{MPP} and MPP will be obtained in any specific temperature and irradiance intensity.

Table 1 Red sun 90 W module

Current at maximum power I_{MP}/A	Voltage at maximum power V_{MP}/V	Maximum power P_{MAX}/ W	Open circuit voltage V_{OC} /V	Short circuit current I_{SC}/A	Total number of parallel cells N_P	Total number of series cells N_S
4.94	18.65	90	22.32	5.24	1	36

Table 2 GA parameters

Number of design variable	Population size	Crossover constant	Mutation rate	Maximum generations
1	27	75%	13%	24

3.2 ANFIS

ANFIS refers to adaptive neuro-fuzzy inference system. An adaptive neural network has the advantages of learning ability, optimization and balancing. However, a fuzzy logic is a method based on rules constructed by the knowledge of experts [20,21]. The good performance and effectiveness of fuzzy logic are approved in nonlinear and complicated systems. ANFIS combines the advantages of adaptive neural network and fuzzy logic. For a fuzzy inference system, with 2 inputs and 1 output, a common rule set is obtained with 2 fuzzy if-then rules by Eqs. (7) and (8). The fuzzy rules can typically be

Rule 1: If x is A_1 and y is B_1; then

$$f_1 = p_1x + q_1y + r_1, \tag{7}$$

Rule 2: If x is A_2 and y is B_2; then

$$f_2 = p_2x + q_2y + r_2, \tag{8}$$

where x and y are the inputs and f is the output. [A_1, A_2, B_1, B_2] are called the premise parameters. [p_i, q_i, r_i] are called the consequent parameters, i = 1, 2. These parameters are called result parameters. The ANFIS structure of the above statements is shown in Fig. 2.

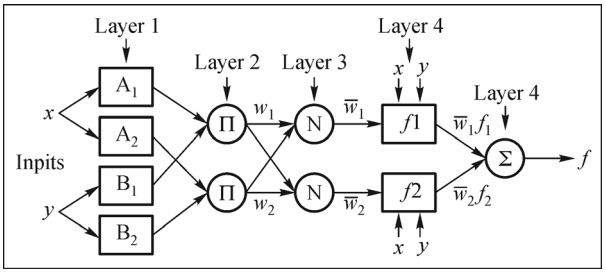

Fig. 2 ANFIS architecture of a 2-input first-order Sugeno fuzzy model with 2 rules

This structure has five layers. It can be seen that the nodes of the same layer have the same functions. The i output node in layer 1 is named as Q_{1i}.

Layer 1: Every node in this layer consists of an adaptive node with a node function. There are

$$Q_{1,i} = mA_i(x), \quad \text{for } i = 1,2, \tag{9}$$

$$Q_{1,i} = mB_{i-2}(y) \text{ for } i = 3, 4, \tag{10}$$

where x (or y) is the input of node i and A_i (or B_{i-2}) is a fuzzy set related to that node. In other words, the output of this layer is its membership value. Each parameter in this layer is regarded as a default parameter.

Layer 2: Each node in this layer is labeled with an "n" and the output of each node is the product of multiplying all incoming signals for that node. These nodes perform the fuzzy AND operation, and there are

$$Q_{2,i} = w_i = m_{A_i}(x)\ m_{B_i}(y) \text{ for } i = 1,2, \tag{11}$$

where the output of each node indicates the firing strength of each rule.

Layer 3: Each node in this layer is labeled with an "N". The nodes in this layer calculate the normalized output of each rule. Then there are

$$Q_{3,i} = \overline{w_i} = \frac{w_i}{w_1 + w_2},\ i = 1,2, \tag{12}$$

where w_i is the firing strength of that rule. The output of this layer is called the normalized firing strength.

Layer 4: Each node in this layer is associated with a node function. Then there is

$$Q_{4,i} = \overline{w_i}\ f_i = \overline{w_i}(p_ix + q_iy + r_i), \tag{13}$$

where w_i is the normalized firing strength of the third layer and $\{p_i, q_i, r_i\}$ are parameter sets of the node i. The parameters of this layer are called "consequent parameters".

Layer 5: The single existing node in this layer is labeled as Σ. It computes the sum of all its input signals and sends them to the output section.

$$Q_{5,i} = \sum_i \overline{w_i} f_i = \frac{\sum_i w_i f_i}{\sum_i w_i}, \tag{14}$$

where $Q_{5,i}$ is the output of the node i in the fifth layer. For this reason, first, all existing rules will be established in layer 1.

This paper uses a hybrid learning algorithm to identify the parameters of Sugeno-type fuzzy inference systems. It utilizes a combination of the least-squares method and the back propagation gradient descent method for training network. A Sugeno-type fuzzy inference system (FIS) structure is applied using Matlab toolbox to produce an FIS structure for the data of PV system based on different proposed Gauss membership functions. The inputs of the ANFIS model can be considered irradiance as a first input and temperature as a second input. Then, the output voltage of the PV module with the ANFIS output voltage is deducted to obtain the error signal. Then, through a PI

controller, this error signal is given to a pulse width modulation (PWM) block. The block diagram of the proposed MPPT scheme is demonstrated in Fig. 3.

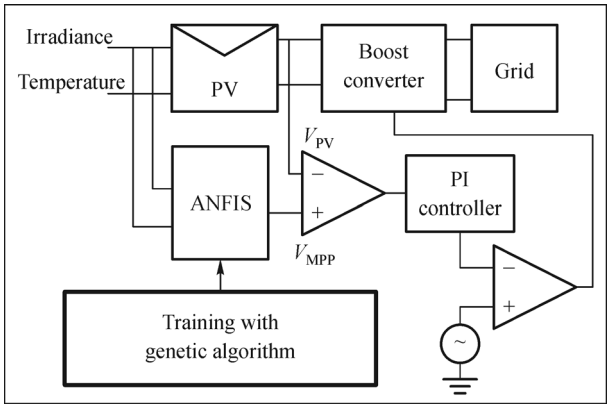

Fig. 3 Proposed MPPT scheme

The PV system is designed in order to obtain optimum values by GA. A set of 360 data of temperature and irradiance are regarded as inputs as shown in Fig. 4(a) and the output is V_{MPP} corresponding to the MPP delivery from the PV panels as depicted in Fig. 4(b). Then these optimum values are utilized for training the ANFIS. By following Fig. 4(a), all input are 360 data in which a set of 330 data are used for training the developed ANFIS model. Besides, a set of 30 data samples are not included in the training. The input temperatures range from 5°C to 55°C in the steps of 5°C and irradiances vary from 50 W/m^2 to 1000 W/m^2 in the steps of 32 W/m^2.

The ANFIS input structure is depicted in Fig. 5 which includes five layers. The inputs of ANFIS can be considered irradiance. The structure shows two inputs of the solar irradiance and cell temperature, which are translated into appropriate membership functions. Three functions for the solar irradiance are displayed in Fig. 6 and three functions for the temperature are illustrated in Fig. 7. They have 9 fuzzy rules in total as exhibited in Fig. 8. These rules have a unique output for each input.

The network is trained for 5000 epochs. After training, the output of the trained network should be very close to the target outputs as shown in Fig. 9. According to Figs. 10 and 11, V_{MPP} is compared with the target values while in Figs. 12, 13 and 14 the output of ANFIS test is compared

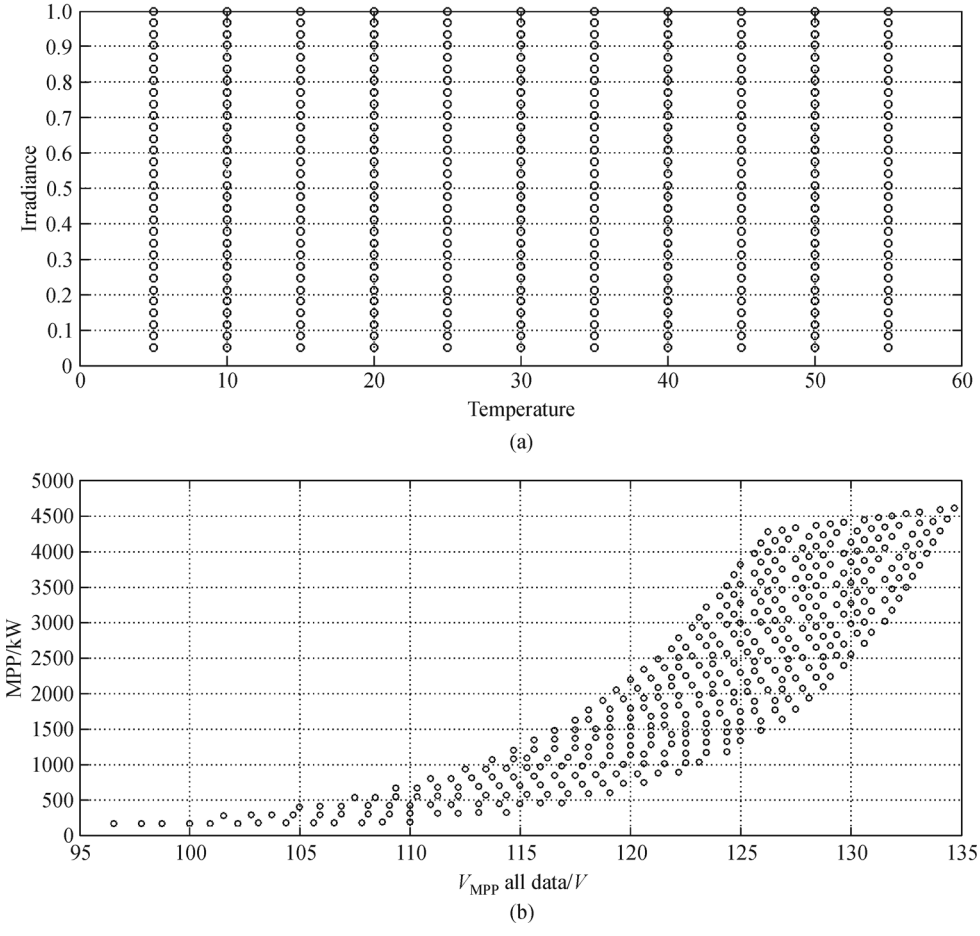

Fig. 4 Data
(a) Inputs data of irradiation and temperature; (b) V_{MPP} corresponding to MPP

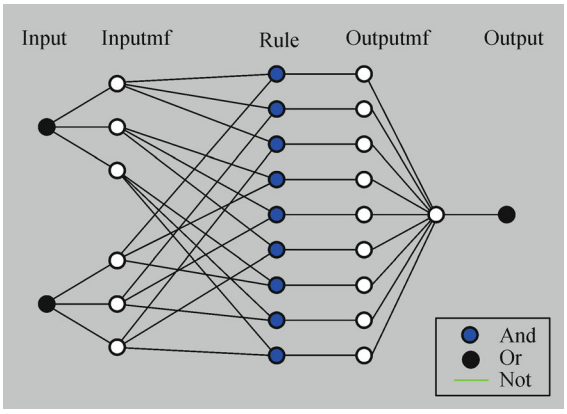

Fig. 5 ANFIS controller structure

with the target values, showing high precision with less than 2% absolute error between estimated voltage and real measured data. This error can be reduced by increasing the number of the training data for ANFIS. The proposed approach has the capability of estimating the amount of generated PV power at a specific time. The ANFIS based temperature and irradiation confirms satisfactory results with minimal error and the generated PV power is optimized significantly with the aids of the GA algorithm.

4 Control strategy (*P*/*Q*)

Synchronous reference calculates quantities of *d*-axis, *q*-axis and zero sequence in two axis rotational reference vector for three phase sinusoidal signal, as illustrated in Fig. 15. The equations are given by Eqs. (15) and (16).

$$\begin{bmatrix} V_d \\ V_q \\ V_0 \end{bmatrix} = \boldsymbol{C}_{dq0} \begin{bmatrix} V_a \\ V_b \\ V_c \end{bmatrix}, \quad \begin{bmatrix} i_d \\ i_q \\ i_0 \end{bmatrix} = \boldsymbol{C}_{dq0} \begin{bmatrix} i_a \\ i_b \\ i_c \end{bmatrix}, \tag{15}$$

$$\boldsymbol{C}_{dq0} = \frac{2}{3} \begin{bmatrix} \cos\theta & \cos\left(\theta - \frac{2\pi}{3}\right) & \cos\left(\theta + \frac{2\pi}{3}\right) \\ -\sin\theta & -\sin\left(\theta - \frac{2\pi}{3}\right) & -\sin\left(\theta + \frac{2\pi}{3}\right) \\ \frac{1}{2} & \frac{1}{2} & \frac{1}{2} \end{bmatrix}. \tag{16}$$

The inverter control model is illustrated in Fig. 16. The active and reactive components of the injected current are i_d and i_q, respectively. For the independent control of both i_d and i_q, the decoupling terms are used. To synchronize the

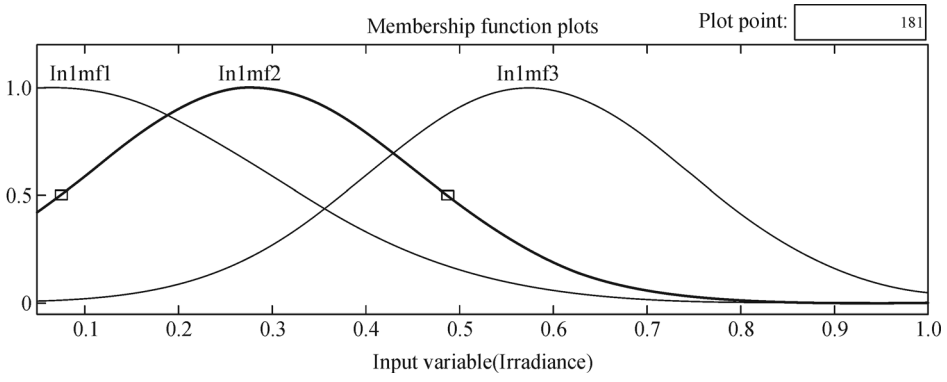

Fig. 6 Solar irradiance membership function for ANFIS

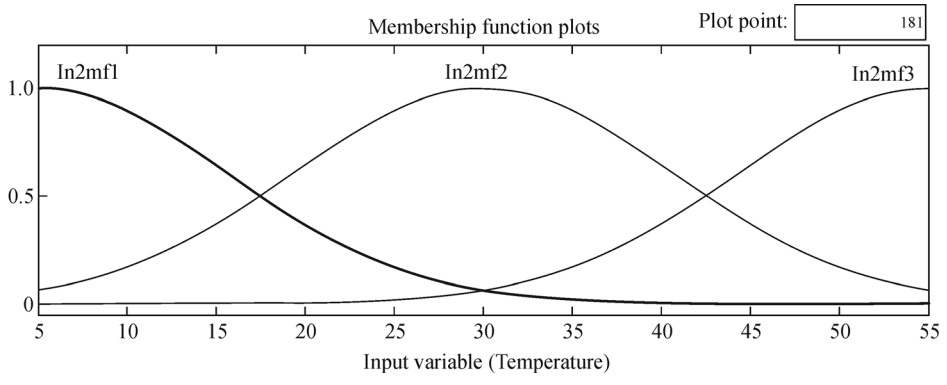

Fig. 7 Temperature membership functions for ANFIS

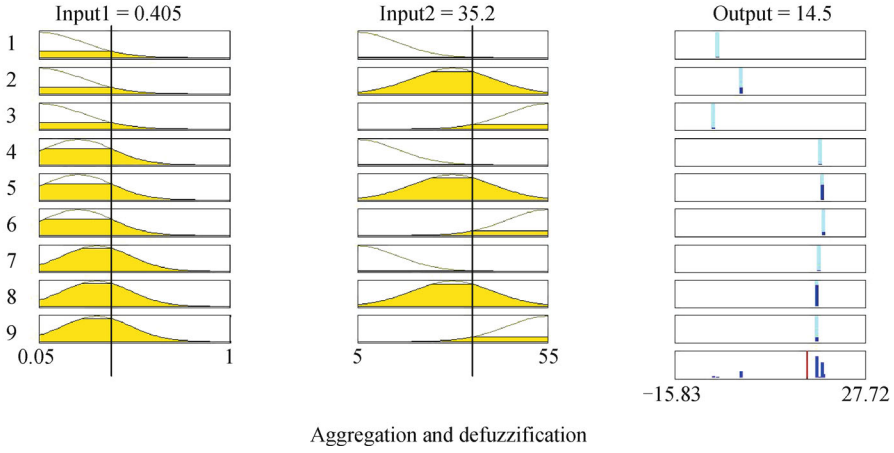

Fig. 8 Fuzzy rules

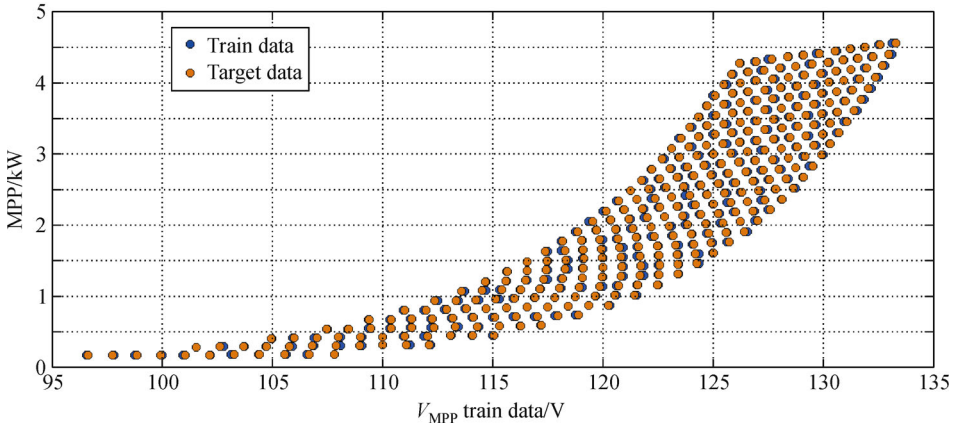

Fig. 9 Output of ANFIS with the amount of target data

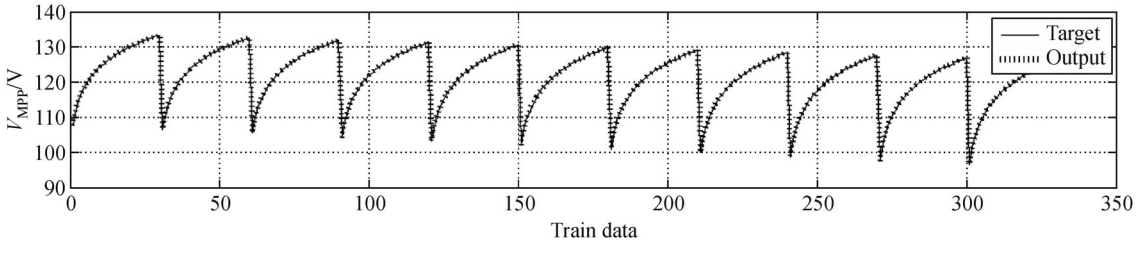

Fig. 10 Output of ANFIS V_{MPP} with the amount of target data

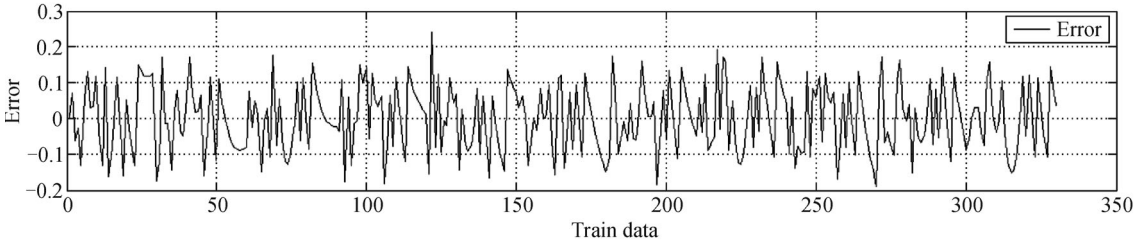

Fig. 11 Total error percentage of V_{MPP} after training data

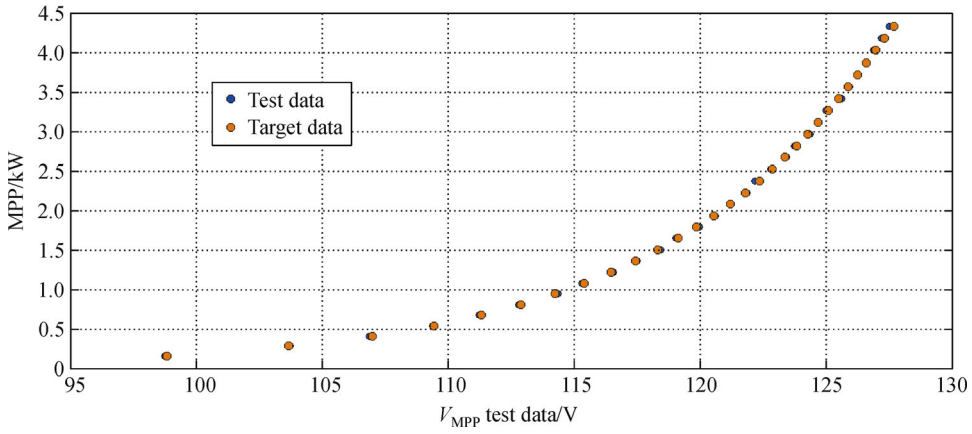

Fig. 12 Output of ANFIS test with the amount of target data

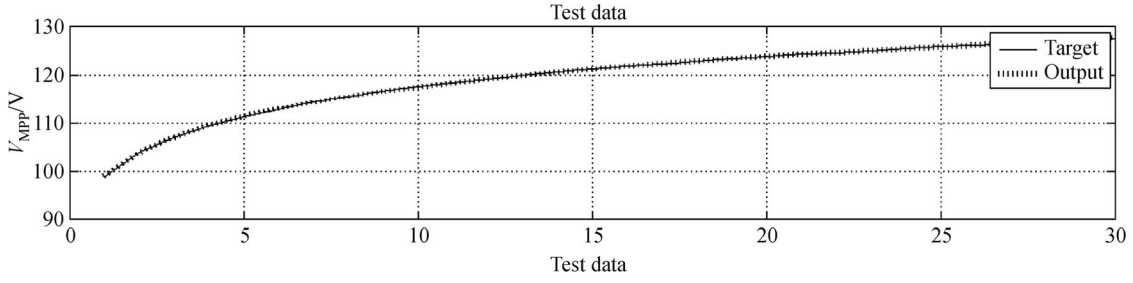

Fig. 13 Output of ANFIS test of V_{MPP} with the amount of target data

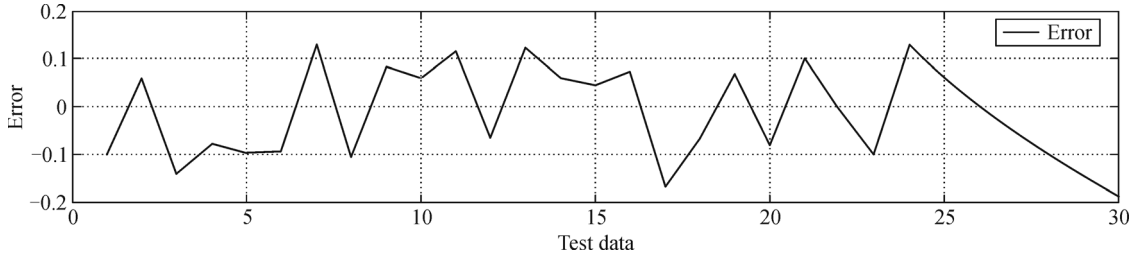

Fig. 14 Error percentage of test data of V_{MPP} after training data

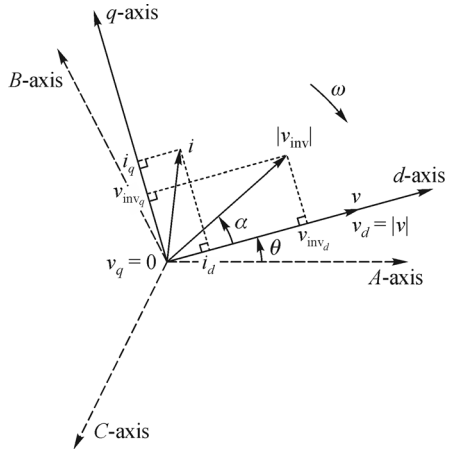

Fig. 15 Synchronous reference machine

converter with the grid, a three phase lock loop (PLL) is used. The PLL reduces the difference between the grid phase angle and the inverter phase angle to zero using the PI controller. It is worth mentioning that the PLL provides the grid phase angle, which is necessary for the Park transformation model ($abc \rightarrow dq$). The goal of controlling the grid side is to keep the DC link voltage in a constant value regardless of production power magnitude. Its output is applied as the reference for the active current controller, whereas the reactive current reference is usually set to zero in normal performance. When the reactive power has to be controlled in some cases, a reactive power reference must be imposed to the control system.

The internal control-loop controls the grid current while the external control loop controls the voltage [26]. Also, the internal control-loop is responsible for power quality

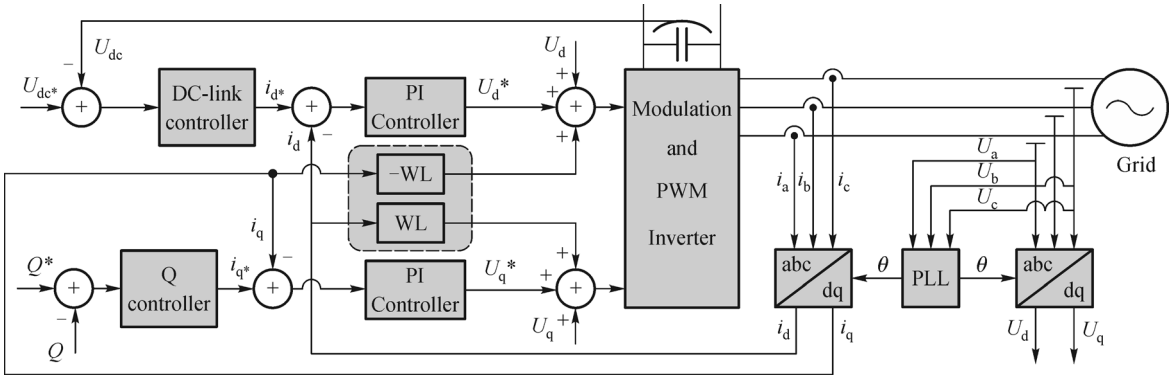

Fig. 16 Inverter control model

such as low total harmonic distortion (THD) and improvement of power quality whereas the external control-loop is responsible for balancing the power. For reactive power control, the reference voltage will be set the same as the DC link voltage. In grid-connected mode, PV module must supply local needs to decrease the power from the main grid. One of the main aspects of P/Q control loop is grid connected and stand-alone function. The advantages of this operation mode are higher power reliability and higher power quality. The active and reactive power are presented by

$$P = \frac{3}{2}(V_{gd}I_d + V_{gq}I_q), \tag{17}$$

$$Q = \frac{3}{2}(V_{gq}I_d - V_{gd}I_q). \tag{18}$$

If synchronous frame is synchronized with grid voltage, the voltage vector is $V = V_{gd} + \mathrm{j}0$, and the active and reactive power may be expressed as

$$P = \frac{3}{2}V_{gd}I_d, \tag{19}$$

$$Q = \frac{3}{2}V_{gd}I_q. \tag{20}$$

5 Simulation results

In this section, simulation results under different terms of operation use with Matlab /Simulink is presented. The system block diagram is shown in Fig. 17. The structure of P/Q strategy is displayed in Fig. 18. The detailed model descriptions are given in Appendix.

To compare the accuracy and efficiency of the four

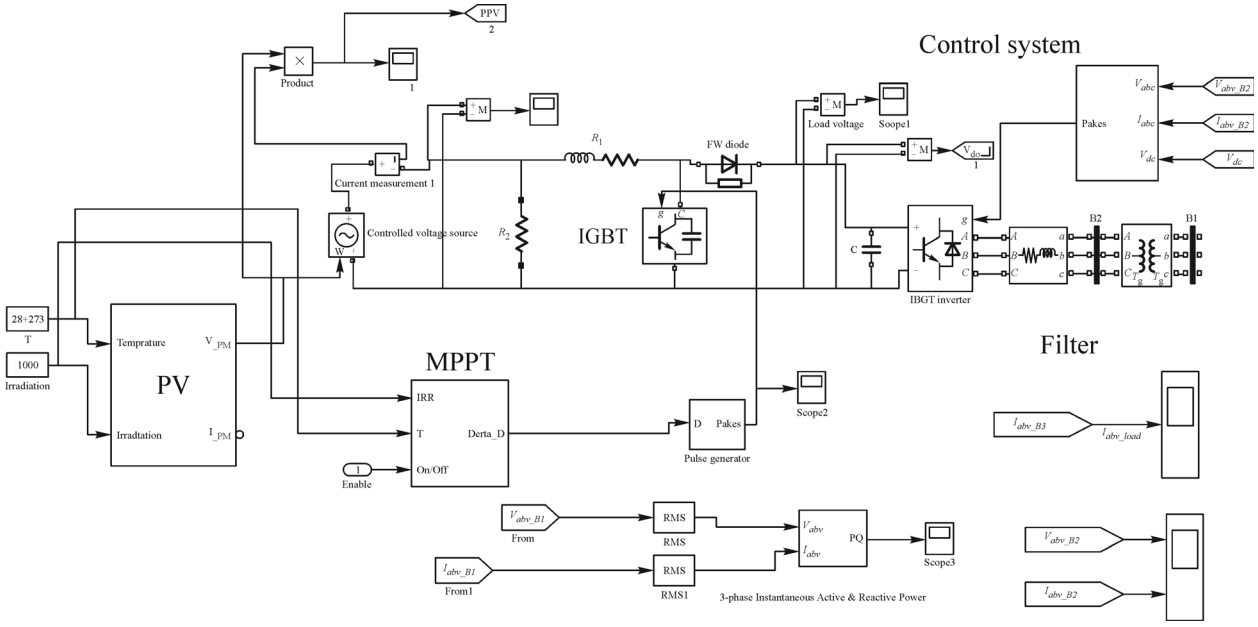

Fig. 17 Case study system

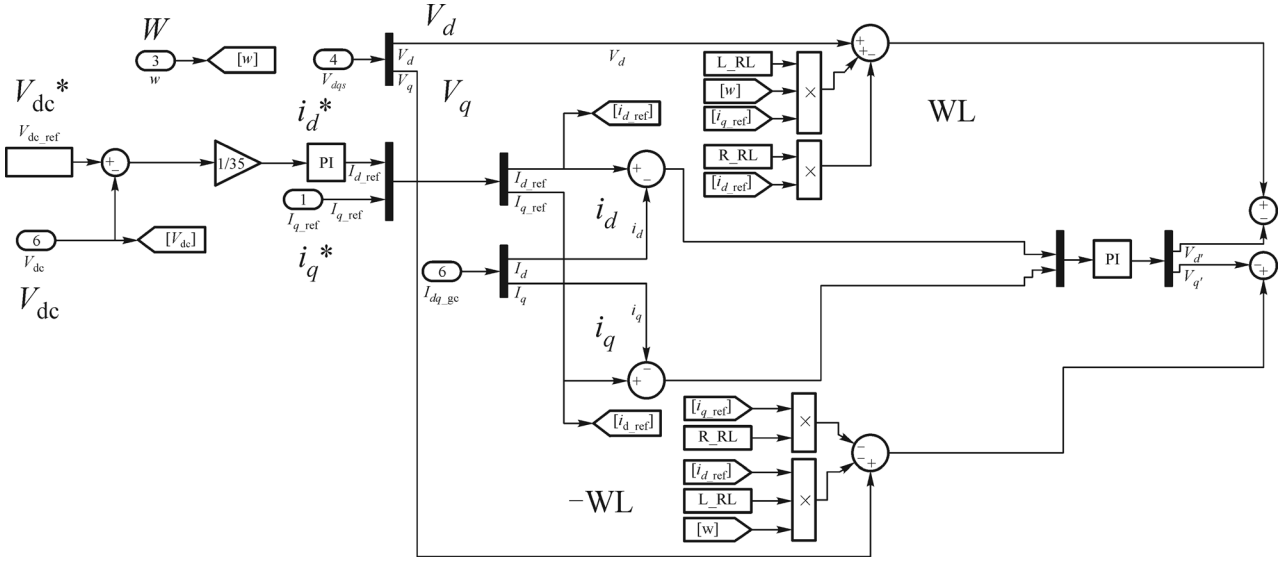

Fig. 18 Structure of *P*/*Q* strategy

MPPT algorithms selected in this paper, Matlab/Simulink is used to implement the tasks of modeling and simulation. The main objective of this case is to investigate the comparative study of MPPT algorithms under variations of irradiance and temperature conditions in the PV system. The system is connected to the main grid that includes the 4.4 kW PV system and the amount of load is 4.4 kW. There is no power exchange between the PV system and the grid in normal condition.

The simulation is conducted for different insolations at a fixed temperature of 25°C as shown in Fig. 19(a). The output voltage and the current of PV are depicted in Fig. 19 (b) and (c), respectively. When the irradiance is increased to $t = 4$ s and $t = 8$ s, it leads to an increase in the output current of PV as shown in Fig. 19(c). The evaluation of the proposed controller is compared and analyzed with the conventional techniques of fuzzy logic, P&O and IC. It is worth mentioning that the proposed MPPT algorithm can track accurately the MPP when the irradiance changes continuously. Besides, this method has well regulated PV output power and it produces extra power rather than aforementioned methods as indicated in Fig. 19(d). Therefore, the injected power from the main grid to the PV system is decreased as demonstrated in Fig. 19(e). The P&O and IC methods perform a fluctuated PV power even after the MPP operating has been successfully tracked.

To precisely analyze the performance of the ANFIS-GA technique, the simulation is conducted for different temperatures at a fixed insolation of 1000 W/m^2 as shown in Fig. 20(a). The grid voltage is indicated in Fig. 20(b). Figure 20(c) shows the variation of the output current of PV. The ANFIS-GA method shows smoother power, less oscillating and better stable operating point than P&O, IC and fuzzy logic. It has more accuracy for operating at MPP, it generates exceeding power and it possesses faster dynamic response than the mentioned techniques as depicted in Fig. 20(d). Consequently, the grid power injection to the PV system declines as illustrated in Fig. 20(e). In the view of power stabilization, the PV power controlled by ANFIS-GA is more stable than that controlled by the conventional methods, which confirms that the PV with the proposed MPPT method can operate in the MPP for the whole range of assumed solar data (irradiance and temperature). The characteristics of the four MPPT techniques are presented in Table 3.

6 Conclusions

This paper discussed the modeling and simulation of a PV system and the implementation of an MPPT algorithm. With the aid of proposed method, the PV system was able to perform and enhance the production of electrical energy at an optimal solution under various operating conditions. To achieve the maximum power from the PV system, the GA-ANFIS technique was used. The GA was used to provide the reference voltage corresponding to the maximum power for any environmental changes. Then optimized values were used for training the ANFIS. For different conditions, the proposed algorithm was verified and it was found that the error percentage of V_{MPP} is from 0.05% to 1.46%. This error could be reduced by increasing the number of the training data for the ANFIS.

By means of the ANFIS-GA algorithm, the disadvantages of previous approaches could dramatically be reduced, the oscillations of power output around the MPP could be decreased, and the convergence speed could be increased to achieve the MPP in comparison with the conventional method. To control the grid current and voltage, a grid-side controller was applied. The inverter

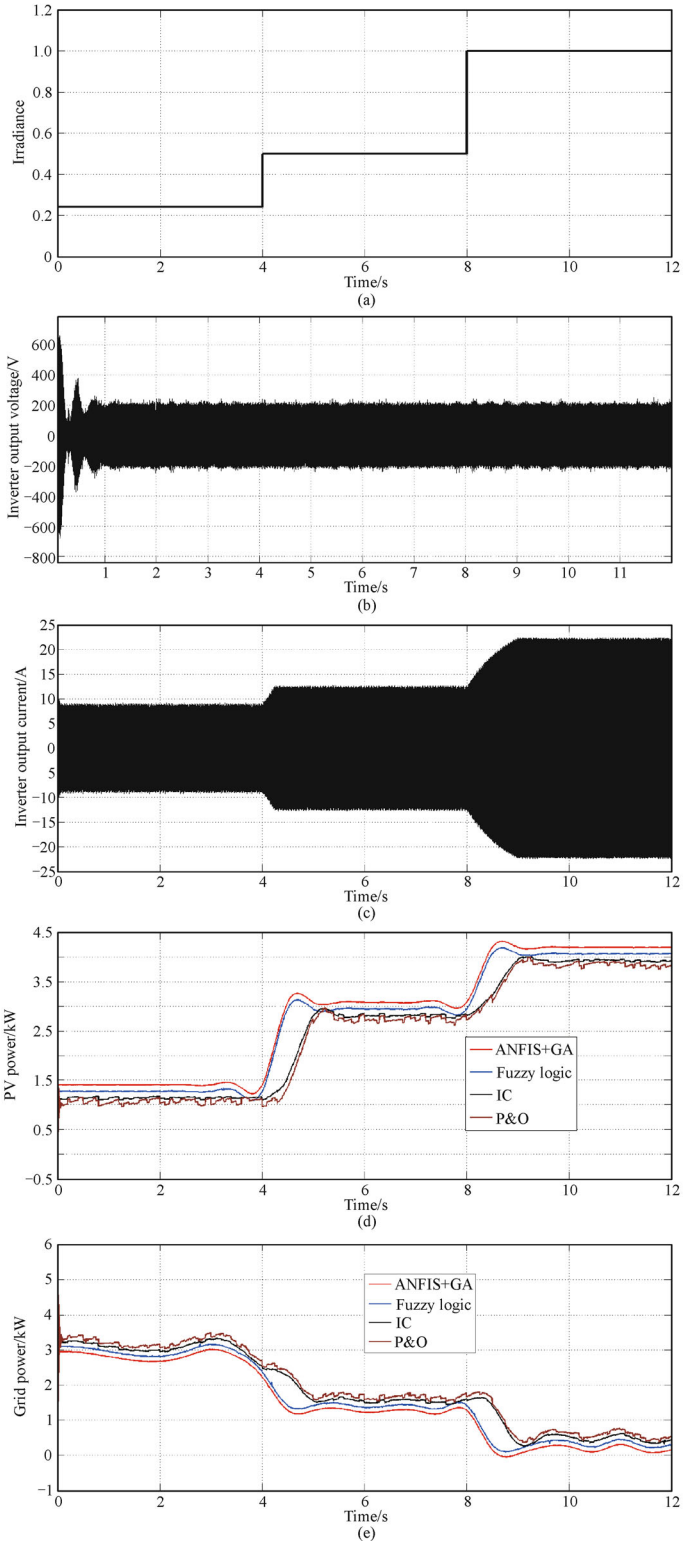

Fig. 19 Simulated results for PV (variation of irradiance) in case 1
(a) Irradiance; (b) inverter output voltage; (c) inverter output current; (d) PV power; (e) grid power

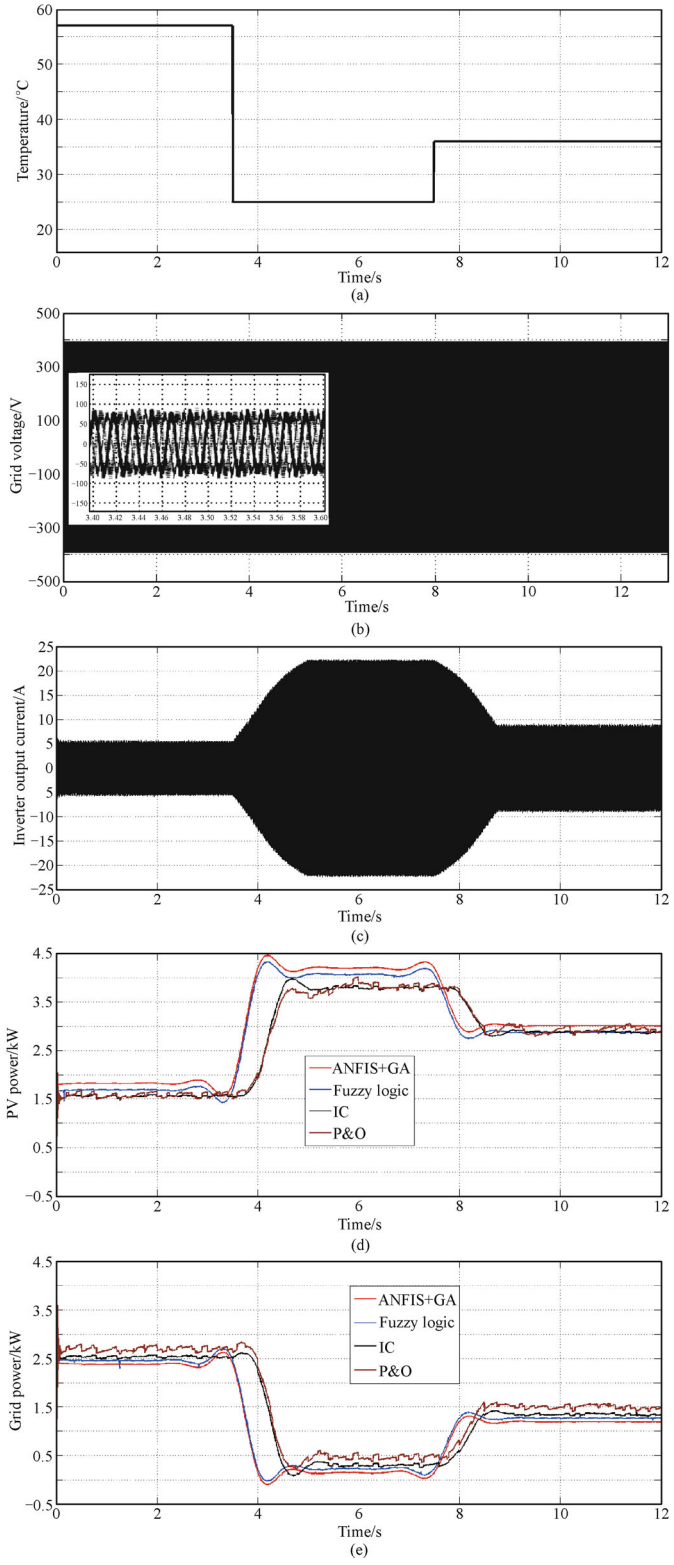

Fig. 20 Simulated results for PV (variation of temperature) in case 1
(a) Temperature; (b) grid voltage; (c) inverter output current; (d) PV power; (e) grid power

Table 3 Characteristics of different MPPT techniques

MPPT techniques	Convergence speed	Implementation complexity	Periodic tuning	Sensed parameters
P&O	Varies	Low	No	Voltage
IC	Varies	Medium	No	Voltage, Current
Fuzzy logic control	Fast	High	Yes	Varies
ANIFS + GA	Fast	High	Yes	Varies

adjusted the DC link voltage while the active power and reactive power were fed by the *d*-axis and *q*-axis, respectively. Finally, by implementing the appropriate controller, the PV system in grid-connected mode could meet the need of load assuredly.

Appendix Detailed description of the model

Photovoltaic parameters: output power = 4.4 kW,
Carrier frequency in V_{MPPT} PWM generator: 4000 Hz and in grid-side controller: 5000 Hz
Boost converter parameters: L = 4.5 mH, C = 970 μF
PI coefficients in grid-side controller: $K_{\mathrm{pVdc}} = 0.4$, $k_{i\mathrm{Vdc}} = 7$, $K_{\mathrm{p}Id} = 8$, $K_{iId} = 700$, $K_{\mathrm{p}Iq} = 8$, $K_{iIq} = 700$, $V_{\mathrm{grid}} = 220$ V.

References

1. Rezvani A, Gandomkar M, Izadbakhsh M, Ahmadi A. Environmental/economic scheduling of a micro-grid with renewable energy resources. Journal of Cleaner Production, 2015, 87: 216–226
2. Izadbakhsh M, Gandomkar M, Rezvani A, Ahmadi A. Short-term resource scheduling of a renewable energy based micro grid. Renewable Energy, 2015, 75: 598–606
3. Salas V, Olias E, Barrado A, Lazaro A. Review of the maximum power point tracking algorithms for stand-alone photovoltaic systems. Solar Energy Materials and Solar Cells, 2006, 90(11): 1555–1578
4. Femia N, Petrone G, Spagnuolo G, Vitelli M. Optimization of perturb and observer maximum power point tracking method. IEEE Transactions on Power Electronics, 2005, 20(4): 963–973
5. Najet R, Belgacem B G, Othman H. Modeling and control of photovoltaic energy conversion connected to the grid. Frontiers in Energy, 2012, 6(1): 35–46
6. Liu F, Duan S, Liu F, Liu B, Kang Y. A variable step size INC MPPT method for PV systems. IEEE Transactions on Industrial Electronics, 2008, 55(7): 2622–2628
7. Altin N. Interval type-2 fuzzy logic controller based maximum power point tracking in photovoltaic systems. Advances in Electrical and Computer Engineering, 2013, 13(3): 65–70
8. Bouchafaa F, Hamzaoui I, Hadjammar A. Fuzzy logic control for the tracking of maximum power point of a PV system. Energy Procedia, 2011, 6(1): 152–159
9. Veerachary M, Senjyu T, Uezato K. Neural-network-based maximum-power-point tracking of coupled inductor interleaved-boost-converter-supplied PV system using fuzzy controller. IEEE Transactions on Industrial Electronics, 2003, 50(4): 749–758
10. Rai A K, Kaushika N D, Singh B, Agarwal N. Simulation model of ANN based maximum power point tracking controller for solar PV system. Solar Energy Materials and Solar Cells, 2011, 95(2): 773–778
11. Chandrasekaran S, Amarkarthik A, Sivakumar K, Selvamuthukumaran D, Sidney S H. Experimental investigation and ANN modeling on improved performance of an innovative method of using heave response of a non-floating object for ocean wave energy conversion. Frontiers in Energy, 2013, 7(3): 279–287
12. Liu F R, Duan S X, Liu F, Liu B Y, Kang Y. A variable step size INC MPPT method for PV systems. IEEE Transactions on Industrial Electronics, 2008, 55(7): 2622–2628
13. Esram T, Chapman P L. Comparison of photovoltaic array maximum power point tracking techniques. IEEE Transactions on Energy Conversion, 2007, 22(2): 439–449
14. Godoy Simões M, Franceschetti N N. Fuzzy optimisation based control of a solar array system. Electric Power Applications, 1999, 146(5): 552–558
15. Huh D P, Ropp M E. Comparative study of maximum power point tracking algorithm using an experimental, programmable, maximum power point tracking test bed. In: Proceedings of 28th IEEE Photovoltaic Specialists Conference. Anchorage, USA, 2000, 1–5
16. Al-Amoudi A, Zhang L. Application of radial basis function networks for solar-array modeling and maximum power-point prediction. IEE Proceedings-Generation, Transmission and Distribution, 2000, 147(5): 310–316
17. Zhang L, Bai Y F. Genetic algorithm-trained radial basis function neural networks for modeling photovoltaic panels. Engineering Applications of Artificial Intelligence, 2005, 18(7): 833–844
18. Hiyama T, Kitabayashi K. Neural network based estimation of maximum power generation from PV Module using environment information. IEEE Transactions on Energy Conversion, 1997, 12(3): 241–247
19. Aldobhani A M S, John R. Maximum power point tracking of PV system using ANFIS prediction and fuzzy logic tracking. In: Proceedings of the International MultiConference of Engineers and Computer Scientists (IMECS). Hong Kong, China, 2008, 19–21
20. Jang J S R, Sun C T, Mizutani E. Neuro-Fuzzy and Soft Computing: A Computational Approach to Learning and Machine Intelligence. Prentice Hall, 1997
21. Patcharaprakiti N, Premrudeepreechacharn S, Sriuthaisiriwong Y. Maximum power point tracking using adaptive fuzzy logic control for grid connected photovoltaic system. Renewable Energy, 2005, 30(1): 1771–1788

22. Vincheh M R, Kargar A, Markadeh G A. A hybrid control method for maximum power point tracking (MPPT) in photovoltaic systems. Arabian Journal for Science and Engineering, 2014, 39 (6): 4715–4725
23. Ramaprabha R, Mathur B L. Intelligent controller based maximum power point tracking for solar PV system. International Journal of Computers and Applications, 2011, 12(10): 37–41
24. Rezvani A, Gandomkar M, Izadbakhsh M, Vafaei S. Optimal power tracker for photovoltaic system using ann-ga. International Journal of Current Life Sciences, 2014, 4(9): 107–111
25. Yang J, Honavar V. Feature subset selection using a genetic algorithm. IEEE Intelligent Systems, 1998, 13(2): 44–49
26. Blaabjerg F, Teodorescu R, Liserre M, Tim-bus A V. Overview of control and grid synchronization for distributed power generation systems. IEEE Transactions on Industrial Electronics, 2006, 53(5): 1398–1409